

Journal of Optoelectronical Nanostructures



Volume 10, Issue 3, Autumn 2025, page 1-20

Research Paper (Pape Type)

Calculation of the energy levels of graphene Nano-discs using the semi-empirical tight-binding method

Masoumeh. Khodagholi, Bahram. Bahrami, Zeynab. Kiamehr* Department of Physics, Tafresh University, Tafresh, Iran

Received: 2025.05.28 Revised: 2025.08.15 Accepted:2025.08.17 Published: 2025.11.30

Use your device to scan and read the article online



Keywords:

Semi-empirical tightbinding (TB) method, Graphene nano-disc, electronic structure, Band gap energy

Abstract:

In this paper, we calculate the band structure of graphene using the empirical tight-binding (TB) method with a first-neighbor approximation and an SP² basis. Subsequently, utilizing the same first-neighbor approximation SP² basis for electron and gap levels, we obtain the energy of graphene nanodiscs (GNDs) with varying radii. As expected, the calculated energy gap decreases with an increase in the radius of the nanodisc. Finally, the energy gap of a nanodisc with a huge radius converges to the energy gap of two-dimensional graphene. Our numerical results indicate that the energy gap is dependent on the shape of the edges and the radius of the GND. Controlling the energy gap by applying an external field is beneficial for optical, infrared, and THz applications. Here, using the empirical tight-binding method for π -electrons, we have estimated the effect of an external electric field on a set of nanodiscs. The application of an external electric field and its impact on the energy gap are key factors in controlling the energy gap of nanodiscs.

Citation: Masoumeh Khodagholi, Bahram Bahrami, Zeynab Kiamehr. Calculation of the energy levels of graphene Nano-discs using the semi-empirical tight-binding method. **Journal of Optoelectronical Nanostructures.** 2025; 10 (3): 1-20

*Corresponding author: Zeynab Kiamehr

Address: Department of Physics, Tafresh University, Tafresh, Iran

Email: z_kiamehr@tafreshu.ac.ir

DOI: https://doi.org/10.71577/jopn.2025.1208072

1. Introduction

Carbon is the main element in biological structures, and the two-dimensional form of carbon is called graphene [1-2]. Graphene's unique properties, including extremely high strength, high transparency to light, excellent electrical and thermal conductivity [3-5], strong excitability of charge carriers, unusual quantum Hall effect [6, 7], and the linear relationship between electron energy scattering at Dirac points and chirality [8], have made this crystalline solid applicable in a variety of fields. These applications include making more efficient transistors and wind turbines [9], creating highly sensitive gas sensors [10, 11], use in optical screens and computers [12], fabrication of supercapacitors [13], and incorporation into medical equipment, earning it the designation of a 'super-material.' The reason for the difference in its properties compared to common two-dimensional semiconductors lies in its distinct band structure. Consequently, charge carriers in graphene exhibit relativistic behavior similar to Dirac's massless fermions, whose dynamics are described by Dirac's equation. For this reason, graphene displays different behavior from normal two-dimensional electron gas from a particle perspective. Graphene is the first truly two-dimensional and stable crystal [14], and due to the aforementioned applications [15, 16], it has garnered significant attention, particularly for the linearity of its energy spectrum at Dirac points [17]. The absence of an energy gap in graphene poses a challenge for controlling electronic properties in graphene-based devices [18], a problem that can be addressed by reducing graphene's size and creating graphene nanodiscs (GNDs). Small strips of graphene are called graphene nanostrips, which involve a limitation in either the width or length of the graphene sheet, whereas a nanodisc is formed by limitations on both sides [19, 20]. A nanodisc is a small segment of twodimensional graphene, with its radius typically on the nanometer scale. Because electrons are confined to a small surface area, their physical properties differ from those of two-dimensional graphene. The efficiency of nanodiscs stems from the adjustment of the wavelength emitted by these structures. This wavelength value is susceptible to the quantum size of the nanodisc. Since the condition of periodic potential is not established for nanodiscs, they lack the translational symmetry of two-dimensional graphene. Due to the non-periodic potential of nanodiscs, energy levels replace energy bands [21, 22].

The tight-binding method is a suitable approach for calculating electron band structure, utilizing the linear combination of atomic wave functions [23]. Although the tight-binding method is a one-electron model, it provides a

foundation for more complex calculations. The first description of the strong bonding in graphene was given by Wallace in 1947. He considered the interaction of first and second nearest neighbors for graphene orbitals but neglected the overlap of wave functions between different atoms [24]. A significant advantage of this method is the derivation of simple formulas for graphene's band structure. The assumptions of this model include the specific separation of energy values and the use of specific functions for an electron in a particular atom. This approach assigns each electron to a specific atomic location, based on the assumption that atoms are sufficiently far apart in solids, and approximates the periodic potential through superposition [25, 26]. The atomic potential definition can be viewed as calculating the Hamiltonian of the entire system using the Hamiltonians of individual atoms, each situated at a lattice point. While using this method is a reasonable approximation for the energy bands of semiconductors, it may not be as accurate for conductors. In the following sections, we will employ the semi-empirical tight-binding method to describe the electronic structure of GNDs. The application of the tight-binding method to nanodiscs is quite straightforward, as it involves disregarding the precise atomic positions at the boundary of the nanodisc and considering them as part of the two-dimensional graphene structure [27, 28].

When discussing the electronic applications of graphene, it's important to acknowledge the issue of electrical contact resistance [29]. This issue, however, can be effectively managed in carbon-based electronic devices [30] by carefully controlling the energy gap of nanostructures. Furthermore, carbon-based devices offer the advantage of being easily recycled and reintegrated into the production cycle. Consequently, manipulating the energy gap is achievable through both structural modifications and the application of external fields. Several methods have been proposed to control graphene's energy gap, each with its own advantages and disadvantages. These methods include: patterning graphene [31, 32], straining graphene [33-37], laterally confining charge carriers in onedimensional graphene nanostructures, and inducing vertical inversion symmetry breaking in bilayer [38, 39] or trilayer graphene [40]. For instance, patterning allows for higher current within the nanostructure, whereas symmetry breaking via an external electric field enables precise adjustment of the energy gap, a feature not attainable through patterning or carrier confinement. Recent theoretical research has highlighted the potential of lateral and simultaneous carrier confinement, combined with inverse symmetry breaking in double-layer nanostructures, for precisely tuning the energy gap [41, 42].

While numerous studies have focused on applying electric fields

perpendicular to nanostructures [33-40], an alternative approach involves considering an intra-surface electric field parallel to the surface. Investigating the effects of this parallel field on the properties of nanostructures is a worthwhile endeavor. A key distinction between these two field orientations is that the parallel field can influence the properties of single-layer systems, whereas the perpendicular field primarily affects the physical properties of multilayers. In this article, we aim to calculate the energy gap of nanodiscs in the presence of an electric field, employing the tight-binding method across a wide range of sizes and field strengths. The article is structured as follows: the next section details the calculation of graphene energy bands using the empirical tight-binding method, considering nearest-neighbor overlaps within the sp2 basis. The third section discusses empirical graphene nanodiscs (GNDs) composed of π bonds, utilizing sp2 orthogonal and non-orthogonal bases for varying radii. The fourth section examines the application of a uniform electric field to π -bonded GNDs. Using the semi-empirical tight-binding method, we will investigate the impact of the applied electric field on the energy levels of nanodiscs with different radii. Finally, the conclusion will be presented in the last section.

2. CALCULATION OF GRAPHENE ENERGY BANDS BY THE SEMI-EMPIRICAL TIGHT-BINDING METHOD

In the tight-binding method, the elements of the Hamiltonian matrix and overlap are sufficient to solve the problem. In this method, the electron wave function is considered a linear combination of atomic orbitals:

$$\varphi_{k}(r) = \frac{1}{\sqrt{N}} \sum_{\mathbf{R}} e^{i\mathbf{k}\cdot\mathbf{R}} \varphi(r - \mathbf{R})$$
(1)

Where $\phi(r-R)$ is the hybrid wave function, k is the electron wave vector, and R is the position vector of the atom in the lattice. Function $\phi(r-R)$ can be considered as a linear combination of individual atomic wave functions:

$$\varphi(\mathbf{r} - \mathbf{R}) = \sum_{n} b_n \, \varphi_n(\mathbf{r} - \mathbf{R}) \tag{2}$$

Here $\varphi_n(\vec{r} - \vec{R})$ is the substituted atomic wave function at the location of the R atom. So, the electron wave function in the crystal can be considered as follows:

$$\varphi_{\vec{k}}(\vec{r}) = \frac{1}{\sqrt{N}} \sum_{n,n} b_n e^{i\vec{k}.\vec{R}} \varphi_n(\vec{r} - \vec{R})$$
(3)

In a crystalline solid, the transfer in the direction of the lattice transfer vectors \vec{R}_i imposes Bloch's theorem, whose form is $\varphi_{\vec{k}}(\vec{r} + \vec{R}) = e^{i\vec{k}.\vec{R}}\varphi_{\vec{k}}(\vec{r})$. Using the

tight-binding wave function, we obtain the eigen-equation $E_n(k)$ of a common value:

$$\sum_{n,R} b_n e^{ikR} \int d^3 x \varphi_m^*(r - R') H_0 \varphi_n(r - R) = E(k) \sum_{n,R} b_n e^{ikR} \int d^3 x \varphi_m^*(r - R') \varphi_n(r - R)$$
(4)

Using Eq.4 energy bands can be obtained by the tight-binding method, in which the summation over the left integral, the elements of the Hamiltonian matrix, and the summation over the right integral, the elements of the overlap matrix are replaced between the atomic wave functions. By using the Hamiltonian matrix and overlap [43] in which the parameters of the tight-binding method in the first neighbor approximation for orthogonal and non-orthogonal basis are replaced by the fitting method [44], we will obtain the graphene band structure. The difference between the non-orthogonal part and the orthogonal part is to ignore the overlaps, and the calculation of the energy bands in this part will be possible only by considering the overlap matrix as a single matrix, in other words, the elements of the overlap matrix are considered equal to Kronecker's delta. The band structure diagram for the most symmetric paths in the first Brillouin zone is shown in Fig. 1. It is good to point out that the overlapping matrix will not only not affect the energy gap, but the linearity of the energy band in Dirac points will remain, but it will affect the energy bands.

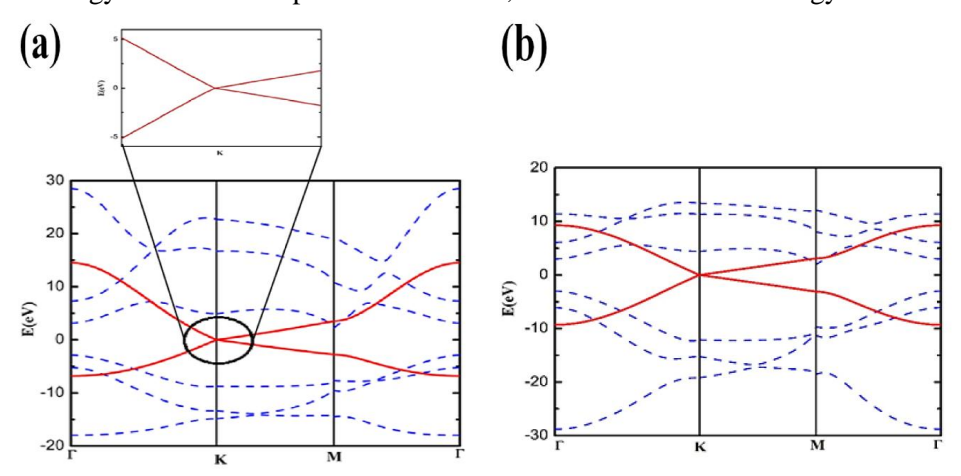


Fig 1. The energy band structures of the $(\pi: red)$, and $(\sigma: dashed blue)$ bonding using the empirical tight-binding method (a) in the non-orthogonal basis, (b) in the orthogonal basis

Bonds π , σ give bands π , π^* (red bands) and σ , σ^* (dashed bands), respectively,

so that bands π and σ (four bands at the bottom of Figure 1), valence bands and bands π^* , σ^* (four bars at the top of Figure 1), are called conduction bands. The most important characteristic of graphene is the linearity of the energy spectrum in the corners of the Brillouin zones around the Dirac points (K point) and it represents the obvious difference between two-dimensional electron gas systems and graphene. The scattering equation for two-dimensional electron gas systems is parabolic, while it is linear for graphene near the Dirac points, and this difference has a significant effect on physical properties such as electrical, magnetic, and optical. We can see that the bands in the orthogonal state will have less energy than in the non-orthogonal state. Also, the comparison of these methods with the strip structure of single-layer graphene using first-principles calculations [45], which uses density functional theory to calculate it, will remind us of the accuracy of our calculations, and there is a good qualitative agreement.

3. CALCULATION OF ENERGY BALANCES OF GNDS BY THE SEMI-EMPIRICAL TIGHT-BINDING METHOD

In this section, the circular GNDs with the origin of coordinates placed in their center will be examined, considering the links π , σ of the closed surfaces. Due to the non-periodic potential of nano-discs, energy balances will arise [45]. To find the energy levels of GNDs, the Schrödinger equation must be calculated. Therefore, a tight-binding wave function of nano-discs is necessary; in other words, the wave function for each nano-disc is a linear combination of individual wave functions of atoms:

$$\varphi(\vec{r}) = \sum_{i=1}^{N_c} \sum_{n=1}^{4} b_{ni} \varphi_n^{\ C}(\vec{r} - \vec{R}_i) + \sum_{j=1}^{N_H} c_j \varphi^H(\vec{r} - \vec{R}_j)$$
 (5)

where N_C is the number of carbon atoms and N_H is the number of hydrogen atoms and 4 is the number of carbon atom orbitals that are added to the selected base. Because hydrogen has only one orbital, no summation will be performed on its orbital. The potential energy for nano-discs is not periodic and we will also use the independent electron approximation according to the previous chapter. With the Hamiltonian assumption $H = \frac{P^2}{2m} + V(\vec{r})$ and a combination of spherical potentials of individual atoms in the nano-disc $V(\vec{r}) = \sum_{i=1}^{N_C} V^C(\vec{r} - \vec{R}_i) + \sum_{j=1}^{N_H} V^H(\vec{r} - \vec{R}_j)$, we have:

$$\sum_{i=1}^{N_c} \sum_{n=1}^{4} b_{ni} \int dx^3 \, \varphi_m^{A^*} (\vec{r} - \vec{R}_j) H \varphi_n^{c} (\vec{r} - \vec{R}_i) + \sum_{j=1}^{N_H} c_j \int dx^3 \, \varphi_m^{A^*} (\vec{r} - \vec{R}_j) H \varphi^H (\vec{r} - \vec{R}_j) \\
= E_r (\sum_{j=1}^{N_H} \sum_{n=1}^{4} b_{ni} \int dx^3 \, \varphi_m^{A^*} (\vec{r} - \vec{R}_j) \varphi_n^{c} (\vec{r} - \vec{R}_i) + c_j \delta_{\vec{R}_i \vec{R}_j}) \\$$
Journal of Optoelectronical Nanostructures. 2025; 10 (3): 1- 20

 $E_{\rm r}$ is the energy level of the nano-disc, the integral on the left side of the Hamiltonian matrix, and the integral on the right side of the overlap matrix. To solve the above equation, due to the non-orthogonality of the desired base, the overlap matrix of the right side of the above equation for carbon-carbon bonds has non-zero non-diagonal elements, but for carbon-hydrogen bonds, non-diagonal elements are equal to zero. The components of the Hamiltonian matrix at the boundary of the nano-disc are made from the product of the wave functions of the carbon atom and the wave functions of the hydrogen atom.

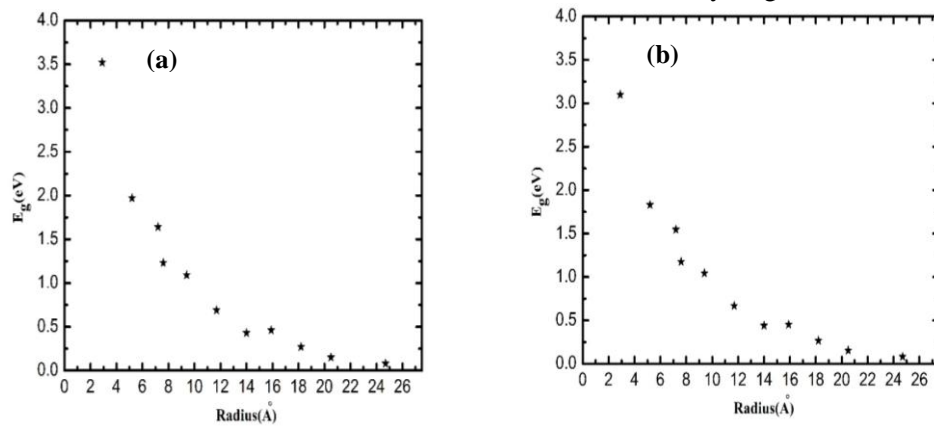


Fig 2. Energy gap in terms of radius and number of hydrogenated GND atoms in sp² (a) non-orthogonal basis, (b) orthogonal basis

Choosing a nano-disc is a way to eliminate the zero energy gap and we can see that, in general, for GNDs, the energy gap changes according to the number of atoms, and its size will have a regular process, that is, with the increase of the radius, which will increase the number of atoms. The energy gap is reduced. Finally, as the radius increases, the energy gap of the nano-disc approaches the energy gap of two-dimensional graphene, which is equal to zero. The effects of quantum confinement are clearly evident in these figures. We can see that in addition to the number of atoms or the size, other factors are effective on the energy levels of nano-discs because it is expected that with the increase in radius, the energy gap of nano-discs will have a regular trend of decreasing and finally tend to zero. In general, what prevents the regular reduction of the energy gap changes will be the surface arrangement and structure of the edges as well as the number of atoms. It can be said that the edges of nano-discs have inherent edge irregularity. For example, in Fig. 2 for a radius of 15.9A° compared to a radius of 14A°, the energy gap has increased, and the reason for that is nothing but the arrangement of the surface and the structure of the edges. We can clearly

see that considering the non-orthogonal base, we will have more changes in the energy gap, and these changes will be more pronounced at smaller radii.

4. CALCULATING THE LEVELS AND ENERGY GAP OF GNDS ONLY CONSIDERING IT BONDS

In this part, we will discuss the formation of Hamiltonian and overlapping elements by ignoring the hydrogen atoms and the σ -bonds of carbon atoms. The exceptional thermal, optical, and electrical properties of graphene are the result of its π -bond coupling [42]. Here, we will have an energy balance with the number of carbon atoms forming the GND, in other words, the dimensions of the Hamiltonian and $N_C \times N_C$ overlap matrices will be. In this case, the nanodisc wave function is written as follows.

$$\varphi(\vec{r}) = \sum_{i=1}^{N_c} b_i \, \varphi(\vec{r} - \vec{R}_i) \tag{7}$$

where N_C is the number of carbon atoms and the potential $V(\vec{r}) = \sum_{i=1}^{N_C} V(\vec{r} - \vec{R}_i)$ of the system is a combination of the spherical potentials of each carbon atom. By performing the same operations as before for the aforementioned nano disc, we reach the following relationship:

$$\sum_{i=1}^{N_c} b_i \int dx^3 \, \varphi^*(\vec{r} - \vec{R}_j) H \varphi(\vec{r} - \vec{R}_i) = E_r \sum_{i=1}^{N_c} b_i \int dx^3 \, \varphi^*(\vec{r} - \vec{R}_j) \varphi(\vec{r} - \vec{R}_i) \tag{8}$$

For both Hamiltonian and overlap matrices, we form the elements by considering only the following values.

$$\left\langle \varphi_{2p_{\pi}}^{A} \middle| H \middle| \varphi_{2p_{\pi}}^{B} \right\rangle = -3.1$$
 and $\left\langle \varphi_{2p_{\pi}}^{A} \middle| \varphi_{2p_{\pi}}^{B} \right\rangle = 0.12$ (9)

where indices A and B represent two neighboring carbon atoms. We will focus our observations only on closed surfaces because if the carbon atoms placed on the edges have a bond with other carbon atoms, they will interact with each other or with the environment and cause the structure to be disturbed. The energy gap for these nano-discs in terms of size and number of atoms is shown in Fig. 3. As before, we can clearly see that the atoms in the closed levels of this system are all individuals, and in general, the energy gap changes according to the number of atoms, and its size will have a downward trend. What prevents the regular and continuous reduction of the energy gap are the arrangement of the surface and the structure of the edges.

5. GND WITH POINT SYMMETRY

In previous calculations, the origin of coordinates was located on a carbon atom at the center of the nano-disk, which formed an asymmetric nano-disk. What allows us to have a symmetric structure is choosing the suitable origin. It is enough to choose the origin as a point with coordinates $((\frac{a_{c-e}}{2}, \frac{\sqrt{3}}{2}a_{c-e}))$ and form the nano-disc around this point (nano-disc with point symmetry). With the help of the information in the previous section, it is easy to calculate the energy gap for each radius, and we will consider its changes according to the number of atoms and size in Fig. 4. In this system, the number of atoms in the closed surfaces will be even, and if the surfaces only contain zigzag edges, then the energy gap will decrease with the increase of these edges, otherwise, the ratio of the number of zigzag edges to the armature is important, will be so that by increasing this ratio, the energy gap will decrease. Also, if the surfaces have the same ratios, then the number of atoms will be the measurement criterion, and the energy gap will be less for a system that has more atoms.

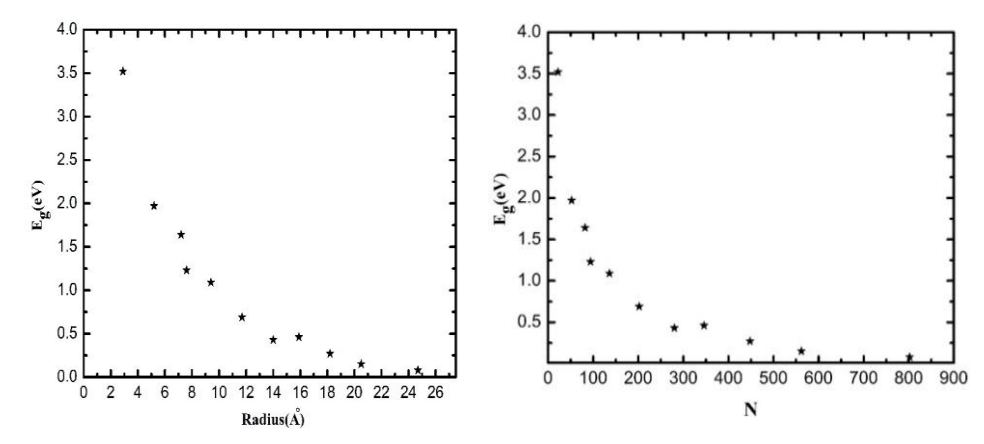


Fig. 3. Energy gap in terms of radiuss and number of atoms of GNDs consisting of π bonds in the non-orthogonal basis

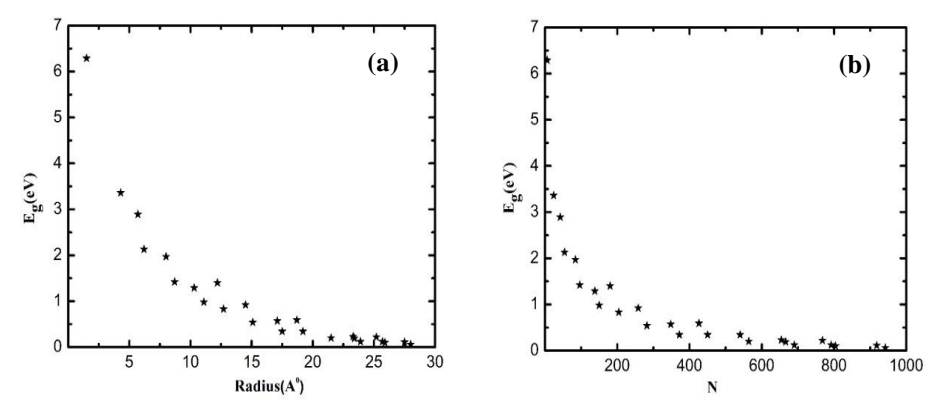


Fig. 4. Energy gap in terms of radius and number of atoms for GNDs with point symmetry in SP² non-orthogonal basis

We have shown the energy of the valence (stars below the dashed line) and conduction (stars above the dashed line) levels in Fig. 5 in terms of the radius of the nano-disc. Both levels have different values and as the radius of the nano-disc increases, they approach zero, which is the energy gap of the graphene crystal.

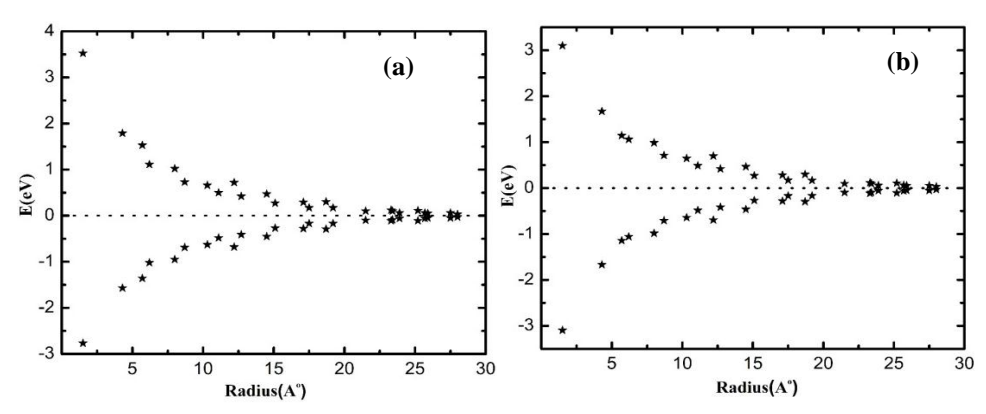


Fig. 5. Energy of valence and conduction levels for different radii for GND with pointsymmetry in SP2 basis (a) non-orthogonal and (b) orthogonal basis

As in the previous discussions, by ignoring the overlaps (Kronecker's delta), the results will be orthogonal. In this base, the levels are completely similar in such a way that we will have a symmetrical diagram, and with the increase of the radius, they both approach zero. Also, by comparing the two orthogonal and non-orthogonal states, as before, it can be seen that the energy gap for a certain radius will be greater in the non-orthogonal state than in the orthogonal state, and this increase in the gap will be more pronounced in smaller radii.

6.CALCULATION OF ENERGY LEVELS OF GNDS IN THE PRESENCE OF AN EXTERNAL ELECTRIC FIELD

In this section, the energy levels of GNDs are investigated using the tight-binding method in the first neighbor approximation in the presence of an external electric field. We know that the Hamiltonian matrix elements for atoms in the unit cell are expressed as $h_{ni} = \langle \varphi_n | \widehat{H} | \varphi_{n+i} \rangle$. Where i=0 for intrasite and i=1 for the first neighbor of the carbon atom. In relation above, the Hamiltonian of the system φ_n is the atomic orbital of the *n*th atom in the unit cell. In the presence of an external field, the Hamiltonian will be of the form $H = \widehat{H_0} + \widehat{U}$. Here $\widehat{H_0}$ is the Hamiltonian of the system in the absence of an external field and \widehat{U} is the potential energy operator for a uniform electric field $\vec{\epsilon}$, which is defined as $\widehat{U} = -e\vec{\epsilon}.\vec{r}$, then we have:

$$h_{ni} = h_{ni,0} + \delta h_{ni} \tag{10}$$

Where $\delta h_{ni} = \langle \varphi_n | U | \varphi_{n+i} \rangle$ and also the applied electric field is weak. By calculating δh_{ni} with the help of the hydrogen atom wave function [45] and carbon atomic number, we see that the electric field applied on the non-diagonal elements of the Hamiltonian matrix will have no effect and only on the diagonal elements (within the site). By substituting of H in relation=H₀+U instead of H₀ in relation $h_{ni} = \langle \varphi_n | \hat{H} | \varphi_{n+i} \rangle$, we can obtain the characteristic Hamiltonian values and use them to calculate the energy gap of nano-discs in the presence of an electric field. In general, the electric field applied to the non-diagonal elements of the Hamiltonian matrix will have no effect and only affect the diagonal elements (within the site). Now, the Hamiltonian matrix for GNDs will be easily organized by applying an electric field. It is sufficient to use the Hamiltonian matrix of GNDs before applying the field by considering only the π bonds and also the nearest neighboring atoms using the sp² approximation that was investigated and calculated in the previous chapter. It is also important to point out that the applied electric field will not affect the overlapping matrix. In this case, we can calculate the energy gap of different nano-discs in the presence of electric fields. Figure 6 shows the energy gap of GNDs with non-point symmetry and point symmetry by applying an external electric field, respectively.

According to Figure 6, for a weak electric field, the energy gap does not change much compared to the case where the field is zero, but the stronger the field, the more obvious the energy gap changes. In general, for the electric field of the gap, the energy first decreases with the increase of the radius similar to the zero electric fields. But for the radius of 20.5A°, the decreasing trend changes, and the energy gap increases and then decreases concerning the zero

electric field. For a nano-disc with point symmetry, it is generally evident that with the application of an electric field, the energy gap of the system decreases compared to the state where no field is applied to the system, and with the increase of the electric field, this reduction of the gap is also maintained for high radii. In Figure 6 by comparing different fields, it can be said that, like the system with non-point symmetry, in the low fields, for example, in the diagram for the regular decreasing process of the energy gap changes according to the radius, it is exactly the same as the case where no field The system is not applied, and with the increase of the field, the failure of the regular decreasing trend of energy gap changes according to the radius of the nano-disc, compared to the case where no field is applied to the nano-disc, will be maintained. In general, we can see in Fig. 6 that the trends of all the points in the form of stars, squares, and triangles are consistent with each other.

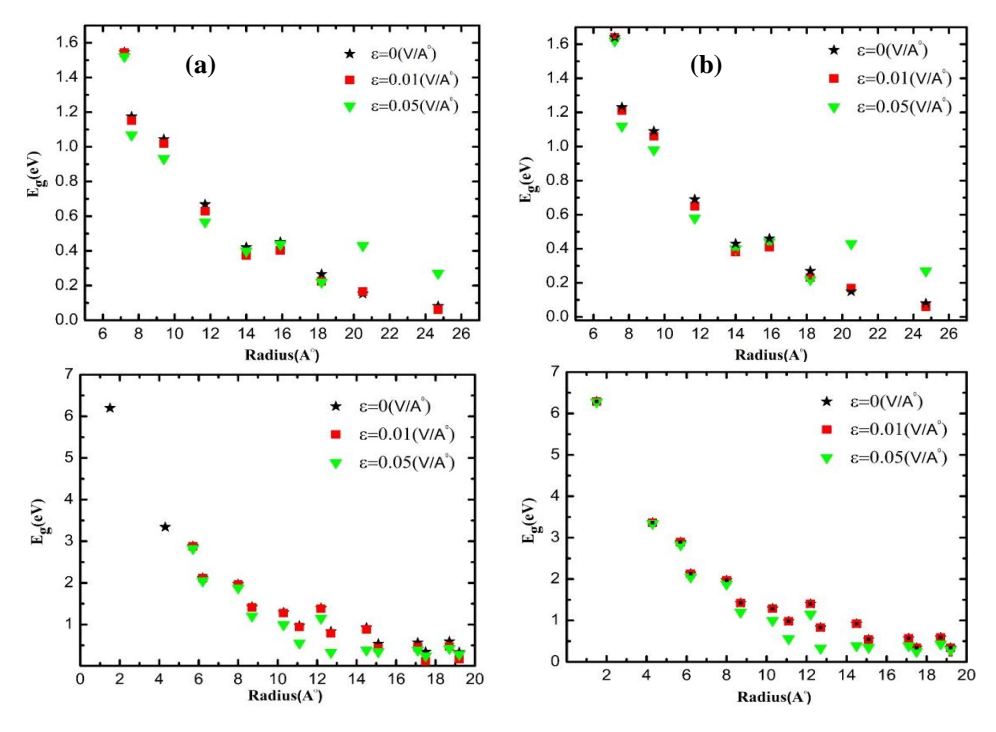


Fig 6. The energy gap of GNDs for different electric fields in the case of (a) non-point and point symmetry with orthogonal sp2 basis and (b) non-point and point symmetry with non-orthogonal sp2 basis

By comparing the orthogonal and non-orthogonal state of this nano-disc, we will see that when no electric field is applied to the system, the energy gap for the non-orthogonal state increases for smaller fields or nano-discs with a smaller radius, and this increase in the gap depends on the radius. It will be more visible in the lower radii. For nano-discs with point symmetry, all the results of the actions mentioned before for the orthogonal state are also true for the nonorthogonal state. For both orthogonal and non-orthogonal basis for the mentioned system, it can be said with certainty that the energy gap decreases with the increase of the electric field compared to the case where there is no electric field. In the following, we will see the energy gap of nano-discs according to the applied electric field. For this purpose, we subject the GND with a certain radius to different fields and investigate the effect of the electric field and the gap changes. The energy gap of GNDs in terms of applied electric fields for the system with non-point symmetry considering overlaps is shown in Fig. 7. The considered radii for these nano-discs are 24.7, 20.5, and 14Å, which are shown in black, blue, and red colors, respectively, in Figure 7.

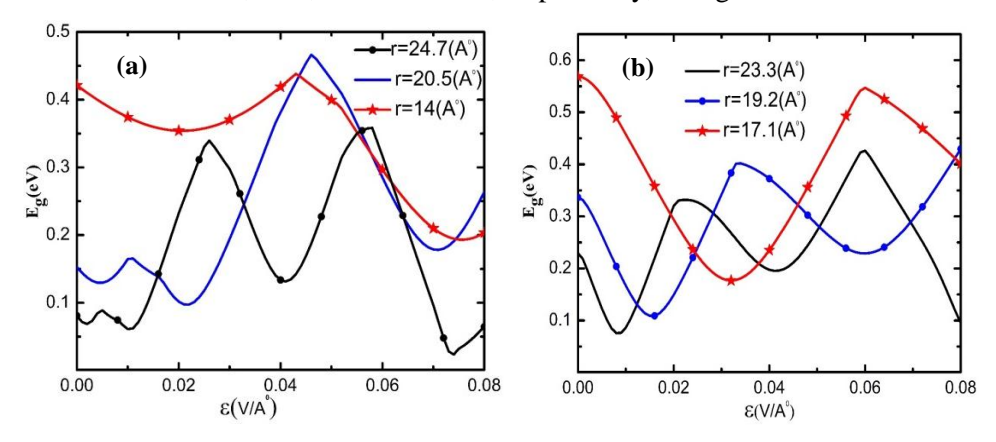


Fig. 7. Energy gap of GNDs with non-orthogonal sp2 basis (a) with non-point symmetry and (b) with point symmetry

We can clearly see that in the nano-disc with non-point symmetry for smaller radii, the process of energy gap changes in terms of the electric field will be more regular. For smaller radii, which are prevented from being drawn in the diagram due to preventing the merging of the diagrams together, the application of the field in the system will cause small oscillations in it so that the gaff changes in terms of the electric field. It will be linear or open curves. For larger radii, where the graph takes the form of successive curves, it can be said that these changes will constantly have ascended and descending points, and these

ascending and descending points occur more often for larger radii. If we repeat the mentioned operation for the orthogonal basis, which means considering the overlap matrix as a unit matrix, we see that applying the overlaps itself will cause changes in the energy gap and that for the applied fields, the energy gap for the states The non-orthogonal will be more, but due to the small differences between these two basis and the presentation problems of the diagrams, we refrain from drawing this diagram for the orthogonal state. Also, in general, in the orthogonal state, more irregularities will rule the system, but since the state non-orthogonal is a more realistic mode for considering such systems, the most attention can be directed to non-orthogonal modes. In the investigation of systems with point symmetry, the energy gap of these nano-discs for different radii and electric fields is also shown in Figure 6. For this system, we have considered the radii of 23.3, 19.2, and 17.1A°, which are shown in black, blue, and red colors respectively in Figure 6. It can be seen that with the increase of the electric field, the energy gap first decreases until it reaches a minimum value, then the energy gap increases until it reaches a maximum value and these changes are repeated. We also see that in the nano-disc with point symmetry for the radii, the smaller the change process of the energy gap in terms of the electric field, the more regular it will be. The changes in the gap in terms of the electric field for small nano-discs will be either linear or open curves. For larger radii, where the graph takes the form of successive curves, we see that these changes will have ascending and descending points, and these ascending and descending points will happen earlier for larger radii. By summarizing all the results and investigations, it can be said that the system with point symmetry will generally have a higher order than the nano-disc with nonpoint symmetry. Finally, it can be said with certainty that choosing a nano-disc and applying an electric field to it is one of the ways to create an energy gap.

7. CONCLUSION

An important goal of nanotechnology is to create structures of materials in which the arrangement of atoms is pre-designed. Finding suitable production techniques in nanotechnology is a topic that has been of great interest to researchers and scientists in recent years. In this article, we calculated the electronic structure of GNDs using the empirical tight-binding method in the first neighbor approximation with orthogonal and non-orthogonal basis. From these approximations, we obtained the energy gap of nano-discs with different radii. It was observed that the energy gap decreases with the increase of the radius of the nano-disc. Finally, with the increase of the radius, the energy gap of the nano-disc will approach the energy gap of two-dimensional graphene.

Nano-disc selection is a method to eliminate the zero energy gaps in graphene. We also observed that for GNDs, the energy gap changes according to its size and will generally have a regular trend. What prevents the regular reduction of the energy gap changes is the arrangement of the surface and the structure of the edges, as well as the number of atoms, and it was observed that the energy gap depends on the geometric shape and structure of the edge. In the end, the effect of the electric field on the energy gap was investigated and we showed that applying the electric field to the nano-disc will be another method to control the energy gap. Our numerical results showed that in nano-discs with a smaller radius, the energy gap change process in terms of the electric field will have less fluctuation than in nano-discs with a larger radius.

As can be seen from Fig. 3, the energy gap of GNDs depends on the radius of the nano-discs, and as the radius of the nano-discs increases, the energy gap of the nano-discs decreases. The effects of quantum confinement are clearly evident in this figure. We can see that in addition to the number of atoms or the size, other factors are effective on the energy levels of nano-discs because it is expected that with the increase in radius, the energy gap of nano-discs will have a regular trend of decreasing and finally tend to zero. In general, what prevents the regular reduction of the energy gap changes will be the surface arrangement and structure of the edges as well as the number of atoms. It can be said that the edges of nano-discs have inherent edge irregularity. For example, a nano-disc with a radius of 14 A° has an energy gap of 0.43 eV, while a nano-disc with a radius of 15.9 A° has an energy gap of 0.46 eV, and this means that the energy gap for a nano-disc with a larger radius is has increased to a nano-disc with a smaller radius. The reason for this increase in the energy gap is related to the shape of the atoms placed on the boundary. The shape of the edge is a combination of zigzag and armchair. For a nano-disc with a radius of 14 A°, the zigzag shape of the edges is more than that of a nano-disk with a radius of 15.9 A°, and vice versa, the armchair shape of the edges is less. In general, the ratio of the number of zigzags to the armchair edges will be important, such that the energy gap decreases as this ratio increases. In other words, the physical properties of GNDs are strongly dependent on the size and topology of their edge structures.

Therefore, we can say that two-dimensional graphene has a zero-energy gap and the energy spectrum is linear in the corners and edges of the Brillouin zones or the Dirac points and the areas close to them, and considering overlaps or ignoring them, on the energy gap and the linearity of the energy spectrum is unaffected. The choice of nano-disc is a method to eliminate the zero-energy gap, and the hydrogen atoms on the surface of the hydrogenated GND and the sigma bonds of carbon atoms will not affect the energy gap. Also, considering

the overlaps or ignoring them will cause changes in the levels and energy gap of the nano-discs in such a way that by choosing the non-orthogonal base, we will witness more changes in the energy gap and as the nano-discs grow, the energy gap will approach the energy gap of 2D graphene. Applying an electric field to the nano-disc will be another method to control the energy gap, and in general, nano-discs with point symmetry have a higher order in the presence of the external electric field than nano-discs with non-point symmetry.

DECLARATION OF INTERESTS

The authors declare that they have no known competing financial interests or personal relationships that could have appeared to influence the work reported in this paper. "No funding was obtained for this study".

REFERENCES

- [1] A. Neto. F. Guinea. N. Peres. K. Novoselov. A. Geim. *The electronic properties of graphene*. Reviews of Modern Physics. 81 (2009) 109. Available: https://journals.aps.org/rmp/abstract/10.1103/RevModPhys.81.109.
- [2] K. Novoselov. A. Geim. S. Morozov. D. Jiang. Y. Zhang. S. Dubonos. I. Grigorieva. A. Firsov. *Electric field effect in atomically thin carbon films*. Science. 306 (2004) 666. Available: https://www.science.org/doi/abs/10.1126/science.1102896.
- [3] T. Mohiuddin. et al. *Uniaxial strain in grapheme by Ramana spectroscopy, G peak splitting, Gruneisen parameters, and sample orientation*. Physical Review B. 79 (2009) 205433. Available: https://journals.aps.org/prb/abstract/10.1103/PhysRevB.79.205433.
- [4] P. Kim. L. Shi. A. Majumdar. P. McEuen. *Thermal transport measurements of individual multi-walled nanotubes*. Physical Review Letters. 87 (2001) 215502. Available: https://journals.aps.org/prl/abstract/10.1103/PhysRevLett.87.215502.
- [5] E. Pop. D. Mann. Q. Wang. K. Goodson. H. Dai. *Thermal conductance of an individual single-wall carbon nanotube above room temperature*. Nano Letter. 6(96) (2005) 100. Available: https://pubs.acs.org/doi/abs/10.1021/nl052145f.
- [6] M. Amirhoseiny, M. Zandi. A. Kheiri. *A Comparative Study of BSF Layers for InGaN Single-Junction and Multi-Junction Solar Cells*. Journal of Optoelectronical Nanostructures. 9(1) (2024) 37-52. Available: https://jopn.marvdasht.iau.ir/article 6220.html.
- [7] V. Singh. D. Joung. L. Zhai. S. Das. S. Khondaker. S. Seal . *Graphene based materials, Past, present and future*. Progress in Materials Science. 56 (2011)

- 1178-1271. Available: https://www.sciencedirect.com/science/article/abs/pii/S0079642511000442
- [8] F. Haldane. *Model for a Quantum Hall Effect without Landau Levels: Condensed-Matter Realization of the parity Anomaly*. Physical Review Letters. 61 (1988) 2015. Available: https://journals.aps.org/prl/abstract/10.1103/PhysRevLett.61.2015.
- [9] T. Sun. et al. *Graphene plasmonic nanoresonators/graphene heterostructures for efficient room-temperature infrared photodetection*. Journal of Semiconductors. 41 (2020) 072907. Available: https://iopscience.iop.org/article/10.1088/1674-4926/41/7/072907/meta.
- [10] S. Damizadeh. M. Nayeri. F. Fotooh. S. Fotoohi. Electronic and Optical Properties of SnGe and SnC Nanoribbons: A First-Principles Study. Journal of Optoelectronical Nanostructures. 5(4) (2020) 67-86. Available: https://jopn.marvdasht.iau.ir/article_4507.html.
- [11] Z. Liu. P. Tang. B. Wu. L. Shi. Y. Li. X. Liu. *Split graphene nano-disks with tunable, multi-band, and high-Q plasmon modes*. Optical Materials. 89 (2019) 18. Available: https://www.sciencedirect.com/science/article/abs/pii/S0925346719300199.
- [12] T. Aghaee. A. Orouji. *Reconfigurable multi-band, graphene-based THz absorber: Circuit Model Approach*. Results in Physics. 16 (2020) 102855. Available: https://www.sciencedirect.com/science/article/pii/S2211379719331341.
- [13] C. Fang. J. Zhang. X. Chen. G. Weng. Calculating the Electrical Conductivity of Graphene Nanoplatelet Polymer Composites by a Monte Carlo Method. Nanomaterial. 10 (2020) 1129. Available: https://www.mdpi.com/2079-4991/10/6/1129.
- [14] M. Hasani. R. Chegell. *Electronic and Optical Properties of the Graphene and Boron Nitride Nanoribbons in Presence of the Electric Field*. Journal of Optoelectronical Nanostructures. 5(2) (2020) 49-64. Available: https://jopn.marvdasht.iau.ir/article_4218.html.
- [15] L. Chernozationskii. P. Sorokin. A. Artukh. *Novel graphene-based nanostructures: physicochemical properties and applications*. Russian Chemical Reviews. 83 (2014) 251. Available: https://iopscience.iop.org/article/10.1070/RC2014v083n03ABEH004367/m eta.
- [16] J. Smith. A. Franklin. D. Farmer. C. Dimitrakopoulos. *Reducing contact resistance in graphene devices through contact area patterning*. ACS Nano. 7 (2013) 3661. Available: https://pubs.acs.org/doi/abs/10.1021/nn400671z.
- [17] F. Haldane. Model for a Quantum Hall Effect without Landau Levels: Condensed-Matter Realization of the Parity Anomaly. Physical Review

- Letters. 61 (1988) 2015. Available: https://journals.aps.org/prl/abstract/10.1103/PhysRevLett.61.2015.
- [18] K. Novoselov. et al. *Two-dimensional gas of massless Dirac fermions in graphene*. Nature. 438 (2005) 197. Available: https://www.nature.com/articles/nature04233.
- [19] S. Mousavi. First–Principle Calculation of the Electronic and Optical Properties of Nanolayered ZnO Polymorphs by PBE and mBJ Density Functionals. Journal of Optoelectronical Nanostructures. 2(4) (2017) 1-18. Available: https://jopn.marvdasht.iau.ir/article-2570.html.
- [20] M. Nishida. Electronic structure of silicon quantum dots: Calculations of energy-gap redshifts due to oxidation. Journal Apply Physics. 98 (2005) 023705. Available: https://pubs.aip.org/aip/jap/article-abstract/98/2/023705/349884/Electronic-structure-of-silicon-quantum-dots?redirectedFrom=fulltext.
- [21] A. Izadparast; P. Sahebsara. *Energy band correction due to one dimension tension in phosphorene*. Journal of Optoelectronical Nanostructures. 2(1) (2017) 59-68. Available: https://jopn.marvdasht.iau.ir/article_2201.html.
- [22] L. Canham. *Silicon quantum wire array fabrication by electrochemical and chemical dissolution of wafers*. Apply Physics Letters. 57 (1990) 1046. Available: https://pubs.aip.org/aip/apl/article-abstract/57/10/1046/974826/Silicon-quantum-wire-array-fabrication-by.
- [23] J. Slater. G. Koster. *Simplified LCAO Method for the Periodic Potential Problem*. Physics Review 94 (1954) 1498. Available: https://journals.aps.org/pr/abstract/10.1103/PhysRev.94.1498.
- [24] J. Deop-Ruano. et al. *Optical Response of Periodic Arrays of Graphene Nanodisks*. Physical Review Applied. 18 (2022) 044071. Available: https://journals.aps.org/prapplied/abstract/10.1103/PhysRevApplied.18.0440 71.
- [25] V. Vuong. et al. Accelerating the Density-Functional Tight-Binding Method Using Graphical Processing Units. The Journal of Chemical Physics. (2023) 5.0130797. Available: https://pubs.aip.org/aip/jcp/article/158/8/084802/2868986.
- [26] N. Melnikov. B. Reser. *Symmetry in the Tight-Binding Method*. Space Group Representations. (2023) 219. Available: https://link.springer.com/chapter/10.1007/978-3-031-13991-8_13.
- [27] P. Pracht. C. Bannwarth. Fast Screening of Minimum Energy Crossing Points with Semiempirical Tight-Binding Methods. Journal of Chemical Theory and Computation. 18(10) (2022) 6370–6385. Available: https://pubs.acs.org/doi/abs/10.1021/acs.jctc.2c00578.

- [28] X. Wu. et al. *Nonadiabatic molecular dynamics simulations based on time-dependent density functional tight-binding method*. The Journal of Chemical Physics. 157 (2022) 084114. Available: https://pubs.aip.org/aip/jcp/article/157/8/084114/2841744.
- [29] J. Liang. et al. *Toward All-Carbon Electronics: Fabrication of Graphene-Based Flexible Electronic Circuits and Memory Cards Using Maskless Laser Direct Writing*. ACS Appl. Mater. Interfaces. 2 (2010) 3310. Available: https://pubs.acs.org/doi/abs/10.1021/am1007326.
- [30] M. Hojatifar. P. Sahebsara. *Tight- binding study of electronic band structure of anisotropic honeycomb lattice*. Journal of Optoelectronical Nanostructures. 1(3) (2016) 17-26. Available: https://jopn.marvdasht.iau.ir/article 2190.html.
- [31] M. Dvorak. W. Oswald. Z. Wu. *Bandgap Opening by Patterning Graphene*. Scientific Reports. 3 (2013) 2289. Available: https://www.nature.com/articles/srep02289.
- [32] S. Choi. S. Jhi. Y. Son. *Effects of strain on electronic properties of graphene*. Physical Review B. 81. (2010) 081407. Available: https://journals.aps.org/prb/abstract/10.1103/PhysRevB.81.081407.
- [33] Y. Li. X. Jiang. Z. Liu. Strain effects in graphene and graphene nanoribbons: the underlying mechanism. Nano Research. 3 (2010) 545. Available: https://link.springer.com/article/10.1007/s12274-010-0015-7.
- [34] R. Ribeiro. V. Pereira. N. Peres. P. Briddon. A. Castro. *Optical properties of strained graphene*. New Journal Physics. 11 (2009) 115002. Available: https://iopscience.iop.org/article/10.1088/1367-2630/11/11/115002/meta.
- [35] V. Pereira. N. CastroNeto. A. Peres. *Tight-binding approach to uniaxial strain in graphene*. Physical Review B. 80 (2009) 045401. Available: https://journals.aps.org/prb/abstract/10.1103/PhysRevB.80.045401.
- [36] L. Chernozationskii. P. Sorokin. *Nanoengineering structures on graphene with adsorbed hydrogen lines*. The Journal of Physical Chemistry C. 114 (2010) 3225. Available: https://pubs.acs.org/doi/abs/10.1021/jp9100653.
- [37] E. McCann. Asymmetry gap in the electronic band structure of bilayer graphene. Physical Review B. 74 (2006) 161403. Available: https://journals.aps.org/prb/abstract/10.1103/PhysRevB.74.161403.
- [38] E. Castro. et al. *Biased bilayer graphene: semiconductor with a gap tunable by the electric field effect.* Physical Review Letters. 99 (2007) 216802. Available: https://journals.aps.org/prl/abstract/10.1103/PhysRevLett.99.216802.
- [39] B. Sahu. H. Min. S. Banerjee. *Edge saturation effects on the magnetism and band gaps in multilayer graphene ribbons and flakes*. Physical Review B.

- 82 (2010) 115426. Available: https://journals.aps.org/prb/abstract/10.1103/PhysRevB.84.075481.
- [40] C. Chang. Y. Huang. C. Lu. J. Ho. T. Li. M. Lin. *Electronic and optical properties of a nanographite ribbon in an electric field*. Carbon. 44 (2006) 508. Available: https://www.sciencedirect.com/science/article/abs/pii/S0008622305004884.
- [41] Y. Son. M. Cohen. S. Louie. *Half-metallic graphene nanoribbons*. Nature. 444 (2006) 347. Available: https://www.nature.com/articles/nature05180.
- [42] P. Vogl. H. Hjalmarson. J. Dow. A Semi-empirical tight-binding theory of the electronic structure of semiconductors. Journal of Physics and Chemistry of Solids. 44 (1983) 365. Available: https://www.sciencedirect.com/science/article/abs/pii/0022369783900641.
- [43] D. Boukhvalov. M. Katsnelson. A. Lichtenstein. *Hydrogen on graphene: Electronic structure, total energy, structural distortions and magnetism from first-principles calculations.* physical Review B. 77 (2008) 035427. Available: https://journals.aps.org/prb/abstract/10.1103/PhysRevB.77.035427.
- [44] E. Leobandung. L. Guo. Y. Wang. S. Chou. *Observation of quantum effects and Coulomb blockade in silicon quantum dot transistors at temperatures over 100 K*. Apply Physics Letters. 67 (1995) 938. Available: https://pubs.aip.org/aip/apl/article-abstract/67/7/938/65715/Observation-of-quantum-effects-and-Coulomb.
- [45] B. Partoens. F. Peeters. *From graphene to graphite: Electronic structure around the K point*. Physical Review B. 74 (2006) 075404. Available: https://journals.aps.org/prb/abstract/10.1103/PhysRevB.74.075404.